Article

Flexible, Stretchable, Tunable, and Switchable DFB Laser

Daniele Eugenio Lucchetta [1,2,*] , Andrea Di Donato [3] , Oriano Francescangeli [2] , Cristiano Riminesi [4,5] , Gautam Singh [6] and Riccardo Castagna [4,5,*]

1   Optoacoustic Lab, Dipartimento di Scienze e Ingegneria della Materia dell'Ambiente ed Urbanistica (SIMAU), Università Politecnica delle Marche, Via Brecce Bianche, 60131 Ancona, Italy
2   Dipartimento di Scienze e Ingegneria della Materia dell'Ambiente ed Urbanistica (SIMAU), Università Politecnica delle Marche, Via Brecce Bianche, 60131 Ancona, Italy
3   Dipartimento di Ingegneria Dell'Informazione (DII), Università Politecnica delle Marche, Via Brecce Bianche, 60131 Ancona, Italy
4   URT-CNR@UNICAM, Università di Camerino (UNICAM), Polo di Chimica, Via Sant'Agostino, 1, 62032 Camerino, Italy
5   CNR, Institute of Heritage Science, Via Madonna del Piano, 10, 50019 Sesto Fiorentino, Italy
6   Department of Applied Physics, Amity Institute of Applied Sciences, Amity University, Noida 201313, India
*   Correspondence: d.e.lucchetta@univpm.it (D.E.L.); riccardo.castagna@cnr.it (R.C.)

Abstract: We are reporting on easily-made, flexible, wearable, and stretchable holographic gratings for tunable distributed-feedback lasers. The laser device is formed by the integration of a reflection volume phase grating in a flexible substrate. The grating is recorded in a photopolymerizable mixture by using optical holography. The photopolymerizing material is a new compound derived from a recently developed mixture which is based largely on haloalkanes and acrylates. An appropriate choice of photoinitiators promotes the photoactivation of the monomers at the writing wavelength of 460 nm. The laser device has a low emission threshold due to the high efficiency of the photopolymerization process at 460 nm. Finally, the amplified spontaneous emission of the device can be continuously tuned by simply bending the film. This peculiarity is promising for the manufacturing of optical pumped tunable organic lasers and flexible displays.

Keywords: distributed-feedback (DFB) laser; holographic reflection gratings; flexible sensors; stretchable displays; free-standing gratings; tunable plastic laser

1. Introduction

The world of interaction between composite polymer materials and light is extremely interesting because it allows for the development of new devices adopting a wide range of previously unimaginable new technologies [1–12]. At the time of writing, flexible electronics is one of the most intriguing research areas, the development of which is essentially based on polymeric composite materials. Flexible, stretchable, and wearable electronics have become increasingly important in today's society. A significant niche of this field is occupied by opto-electronics and, as a consequence, an important role is played by distributed-feedback lasers (DFB) [13]. In recent years, the evolution of flexible DFB lasers [14] has further amplified the perspectives of this sector. As an example, in [15], conjugated polymers are used to produce flexible DFB lasers emitting at multiple wavelengths when appropriately stretched. Recently, we presented a novel polymer composite mixture suitable for use in high-density optical data storage and in DFB lasing, due to its very high transparency, high-diffraction efficiency, and the resolution of the recorded volume phase reflection gratings [16,17]. The mixture is based on a combination of multi-acrylate dipentarythritol-hexa-acrylate (DPHA) and a low refractive index material, usually a haloalkane. The presence of haloalkanes induces a lowering of the average refractive index of the mixture, an increase in the sample transparency in the visible (Vis)-region, a better phase separation process, and a lowering of the viscosity, which

can be inserted into micrometric-sized devices even at environmental temperature. Here, we intend to further exploit its characteristics and propose a very easy-to-make, flexible, and wearable holographic device that can produce highly efficient and frequency-tunable and/or -switchable DFB lasers. The central principle is the insertion of a polymerized material containing a high-resolution reflection grating in a double-layered scotch tape flexible film. The first layer of scotch tape is used to peel off the DFB grating from the recording glass support, while a second layer covers and seals the entire structure in order to protect it from possible aerobic degeneration. At the same time, this particular configuration makes it more manageable and suitable for tunability in terms of DFB frequencies emission and intensity (tunable and/or switchable DFB laser).

2. Materials and Methods

2.1. Materials

DPHA, butyl-bromide (BB), hexyl-bromide (BH), 6-Oxocamphor (6OC), and RH6G are purchased from Merck, Darmstadt, Germany.

2.2. Methods

2.2.1. Holographic Mixture

The procedure is similar to that detailed in the Methods section of Ref. [13]. In brief, BB (20%, w/w), BH (10%), DPHA (c.a. 68%), 1.9% 6OC, and 0.05% RH6G are blended together till a homogeneous pale orange color is obtained. After that, the mixture is stirred at room temperature, in dark aerobic conditions for 6 days and stored for 90 days before being used.

2.2.2. Cell Preparation

The above prepared mixture is then inserted by capillarity between two glass slides separated by a thickness of ≈ 50 μm.

2.2.3. Hologram Recording Set-Up

The recording set-up is shown in Methods of Ref. [13]. In this work, we used a different polymerizing continuous laser source, a Coherent Genesis MX-460 single longitudinal mode (SLM) operating at λ_w = 460 nm. The irradiation time is 1.2 s.

#### 2.2.4. Flexible Grating Preparation

After the grating recording, the whole structure (including the material surrounding the grating area) is further polymerized with the help of a high-power UV-A lamp (λ = 365 nm; P = 0.5 W) placed directly in contact with the glasses containing the sample for one minute. After post-polymerization, the cell is opened and the polymer film strip—containing the DFB grating—is peeled-off with the help of a transparent scotch tape. Once the polymer grating strip is attached on the scotch tape strip, a further tape layer is used to seal the polymerized structure. The final result is a DFB grating inserted between two transparent scotch tape strips. The thus prepared free-standing film is finally clamped in the optical pumping setup.

2.2.5. Pumping and Detection Set-Up

The pumping set-up is made by a Nd-YAG pulsed laser operating at λ = 532 nm τ = 4 ns. The pulsed light impinges at 45° to the clamped free-standing sample containing the photo active mixture. The light emitted by the device is selected and amplified by the presence of the DFB grating and collected by a thin lens at the entrance of an optical fiber connected to a spectrometer.

3. Results and Discussion

Figure 1 shows the transmission spectrum of the recorded DFB structure. The final position of the reflection peak depends on the recording angle and on the shrinkage phenomenon as will be discussed below in the text. The normalization of the transmitted signal is made outside of the grating area. This explains a transmission higher than 100% in the left region of the spectrum, since the transparency in the grating area is higher than that in the other regions of the sample. In the inset of the same figure we report, in black, the transmission spectrum of the polymerized free-standing film (see the Section 2) and, for comparison, in blue, the transmission spectrum of the flexible polymerized film confined between two transparent scotch tape strips. The spectra slightly differ from one another, being composed of polypropylene and acrylate. Irradiation at the wavelength $\lambda_w = 460$ nm for 1.2 s, gives an efficient phase separation process in our mixture allowing the recording of reflection gratings with a 50% value of diffraction efficiency.
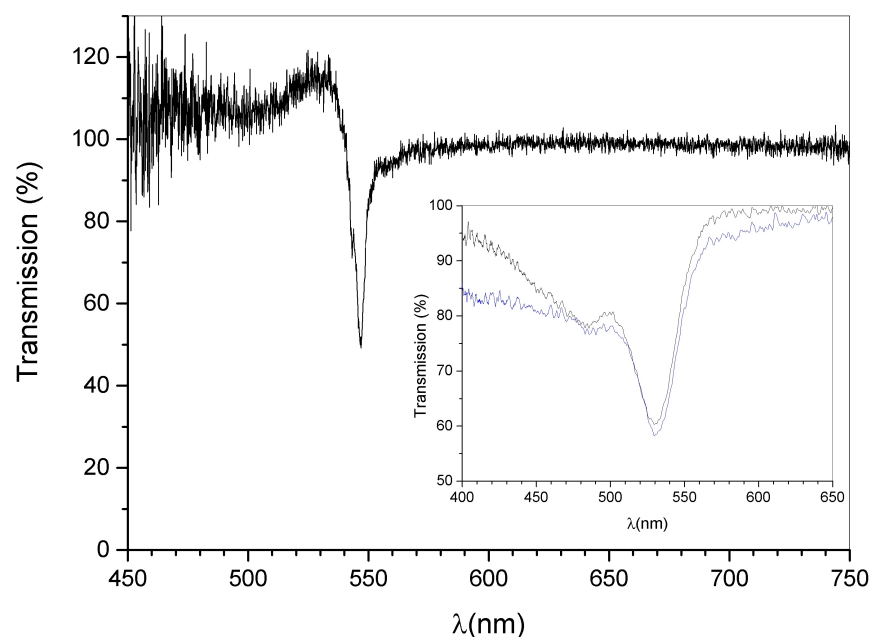

Figure 1. Transmission spectrum showing the normalized reflection peak at the end of the recording process. The normalization is performed outside the grating area. This explains a transmission higher than 100% in the first region of the spectrum. In the inset we report, in black, the transmission spectrum of the polymerized free-standing film and, for comparison, in blue, the transmission spectrum of the flexible polymerized film confined between the two transparent scotch tape strips.

The recording process is however affected by a considerable shrinkage. For this reason, it is essential to monitor in real time the growth of the reflection peak and its displacement (blue-shift) in order to stop the irradiation when the peak reaches the maximum value of diffraction efficiency. A typical behavior is shown in Figure 2. Reported in this figure is the growth of the reflection peak after ≈2 s of irradiation. As it can be seen, the peak grows up to a maximum value (after ≈1.2 s) and after that the diffraction efficiency decreases and a parasite grating appears [16]. For this reason, we decided to stop the irradiation after 1.2 s. For a more complete treatment of the shrinkage phenomenon please see ref [18–21] and references quoted therein.

An amplified spontaneous emission (ASE) effect [22–25] can be easily seen by pumping the sample outside the grating area, see Figure 3. This effect is typical when a laser dye such as the rhodamine 6G (R6G) is used. R6G, like many other laser dyes, is characterized, under excitation, by a complex energy levels diagram involved in which are transitions between singlet and triplet states. The electronic levels are wide in energy due to a continuum of vibrational, rotational, and solvent states. The diffracted energy of a grating containing

a small amount of R6G (typically in the range 10^{-2}–10^{-4} mol) depends on the square of the incident energy. For high values of the impinging energy a saturation of the diffracted energy connected with the saturation of the excited state population is observed. IN deep information and energy level diagrams of R6G can be found in Ref. [26].
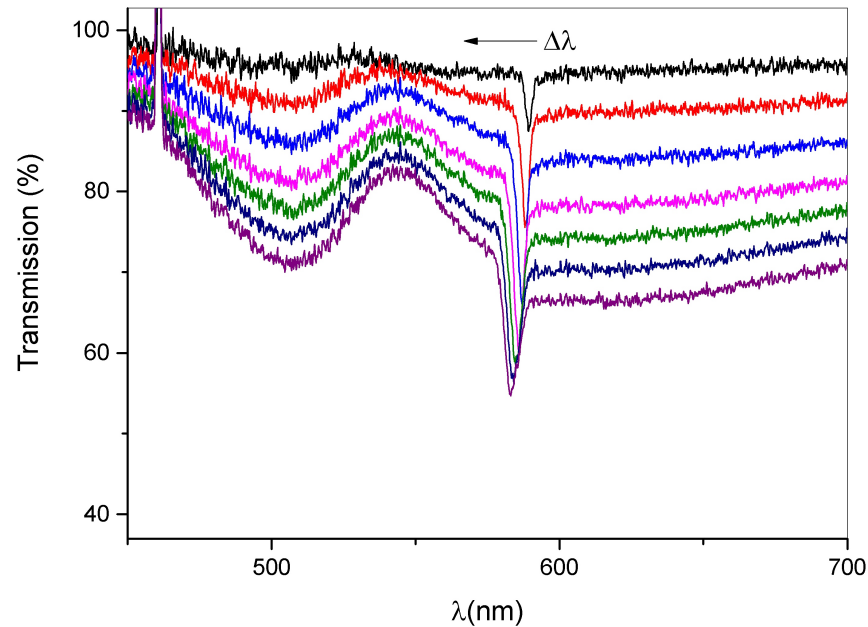

Figure 2. Real-time growth of the reflection peak under irradiation at $\lambda = 460$ nm. The acquisition time is 100 ms. The first peak (black curve) appears at t = 0.15 s. The total irradiation time is ≈2 s and the maximum of diffraction efficiency is obtained after ≈1.2 s. The blue-shift $\Delta\lambda$ of the reflection peak is due to the shrinkage under irradiation.
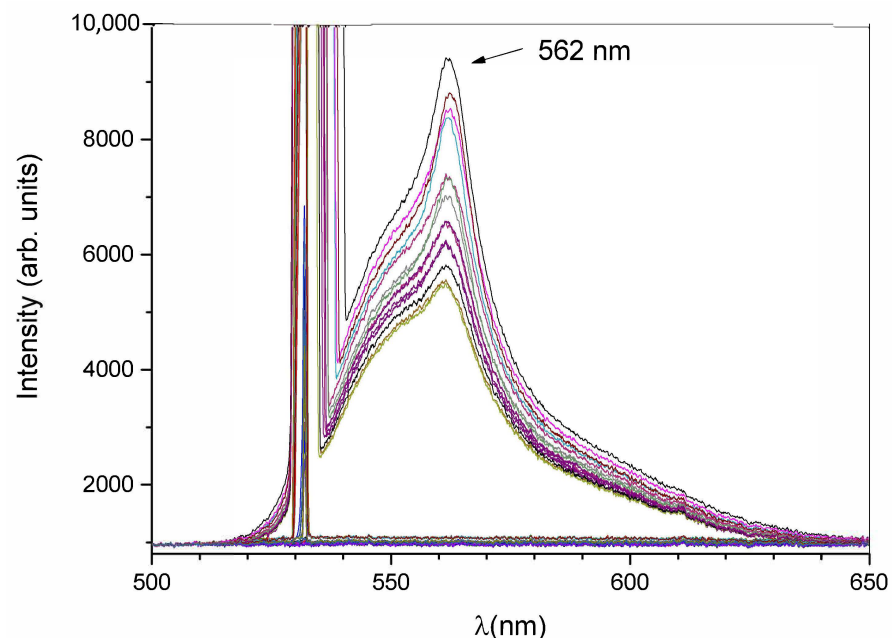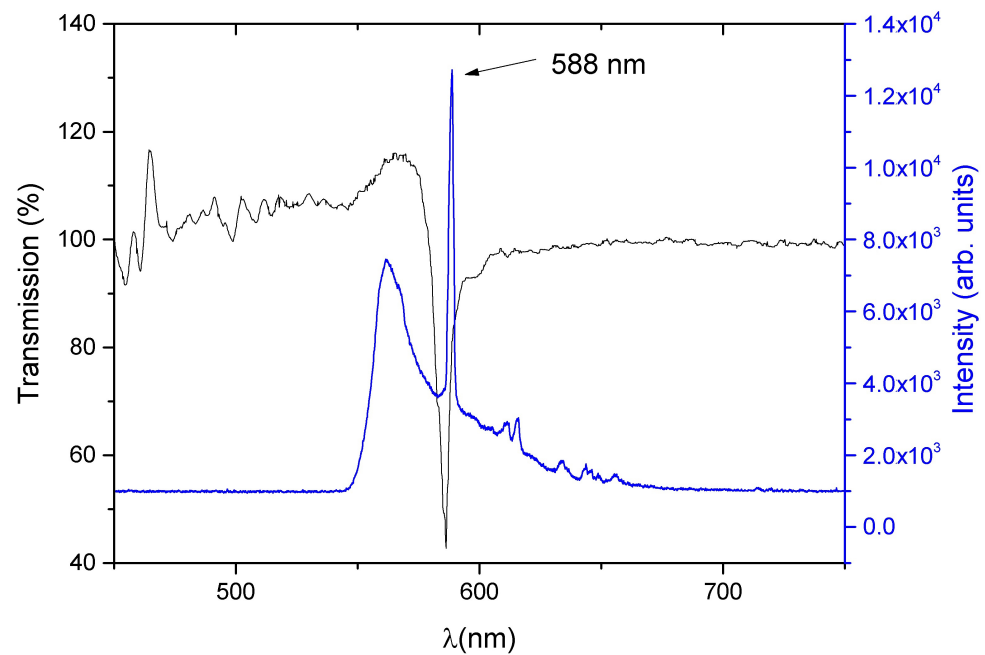

Figure 3. The ASE effect is observed by pumping the free-standing film outside the grating area. The peak on the left side is due to the pumping beam. The wide peak on the right side has a full width at half maximum (FWHM) of about 5 nm and is due to the presence of the R6G dye. The range of fluences used is 10–80 mJ/cm^2, the ASE threshold is located at ≈15 mJ/cm^2. Irradiation wavelength $\lambda = 532$ nm, pulse duration $\tau = 4$ ns.

It is important to note that the full width at half maximum (FWHM) of the emitted light remains stable at 5 nm for the whole set of measurements. Figure 4 reports the emission spectra of our device for values of the irradiation energy ranging from 4 to 20 mJ which when an irradiated area has a 3 mm radius corresponds to $\approx$15–70 mJ/cm^2. In the inset of the same figure, the intensity of each single peak as a function of the pumping energy is reported. The shown behavior does not suggest any lasing effect.
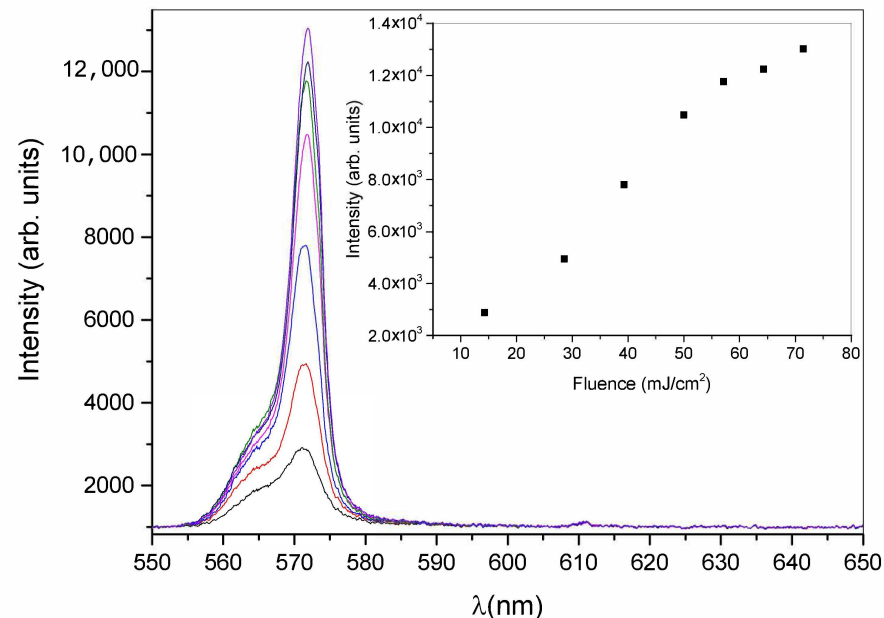

Figure 4. The ASE effect is observed by pumping the free-standing film at λ = 532 nm and τ = 4 ns outside the grating area. In the inset the fluence values used to pump the free-standing structure.

By properly setting the writing angle and the exposure time of the recording source, a reflection peak showing a 50% diffraction efficiency, centered around 585 nm, can be recorded. The minimum of the peak located at 585 nm is far from the naturally growing peaks of our mixture containing the R6G dye. By pumping the system with a pulsed Nd-YAG source a clear laser effect can be detected at 588 nm as shown in Figure 5. Lasing happens on the edge of the photonic bandgap where the density of states (DOS) is higher. The DOS of a one-dimensional periodic structure is defined as: $D(\omega) \propto \int dk \delta[\omega - \omega(k)] = \left| \frac{d\omega}{dk(\omega)} \right|^{-1} = \frac{1}{v_g}$. It shows Van Hove singularities at the two edges of the photonic bandgap [27,28]. The singularity becomes a narrow sharp peak in the DOS that improves ASE bringing to lasing once a threshold of $\approx$3.5 mJ/cm^2, in our specific case, is reached. From a physical point of view, at the band edges, the photons experience multiple reflections causing them to move collectively slowly. This behavior allows for large population build-up and an increase in the optical path length. The presence of the R6G, ensures light amplification and lasing on one of the edges of the photonic stop band. The emitted light satisfies the condition of constructive interference, see Refs. [29–31]. Above a threshold value the light emitted from the excited R6G molecules is amplified in a resonant way and finally laser emission occurs. Narrowing of the emission band of the R6G is observed by monitoring the behavior of the emission peak of the band as a function of the excitation energy. The results are reported in Figure 6 which reports the emission spectra of the DFB grating when pumped with energies in the range 3.5 mJ/cm^2–$\approx$70.0 mJ/cm^2. The inset of the same figure shows the behavior of the height of the peaks as a function of the fluence. The analysis of this figure shows a nonlinear behavior characterized by an abrupt change of the slope at $\approx$10 mJ/cm^2 directly connected to the appearance of the laser emission.

Figure 5. Typical lasing effect (in blue) observed by pumping the grating structure with a fluence of ≈40 mJ/cm^2, λ = 532 nm and τ = 4 ns. In black the reflection peak recorded in the active mixture.
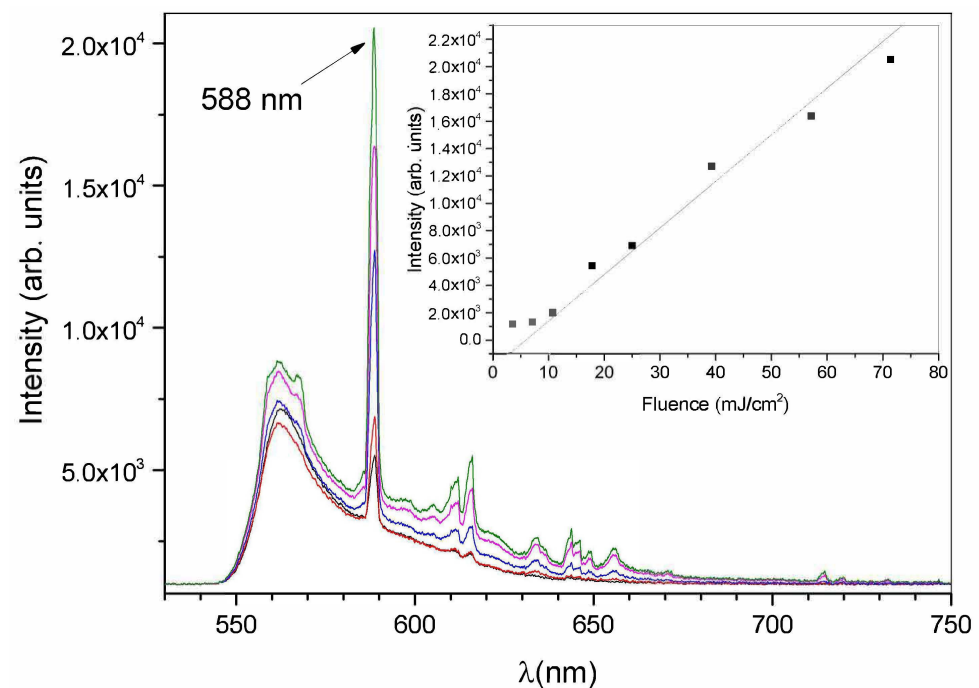

Figure 6. Lasing from the free-standing DFB structure for different values of the impinging energy. The energy values are reported in the inset. The laser threshold is around ≈3.5 mJ/cm^2.

During our experiments, we also observed an interesting phenomenon linked with the bending of our free-standing film. The phenomenon involves the mechanical tuning of the device obtained by simply stretching the film along the directions indicated by the red arrows in the sketch of Figure 7. By starting with the film bent in the position indicated by the number 1, and moving through different bending states along the blue arrow until a straight film is obtained, we noticed that, by pumping outside the grating area, the emission changes from 568 to 572 nm. A similar behavior is obtained by simply rotating the bent sample. We believe that the change in the emitted wavelength is linked to variations in

the impact cross section of the pumping source when the bend conditions or the rotational angle change. The observed variation in the emitted wavelength could also be due to a bend-induced change of the grating pitch or simply by a non uniformity of the grating structure among the irradiated area. This situation can only be investigated by an accurate SEM analysis of the sample cross section. Connected with the changes in the emitted wavelength we observe also a remarkable growth of the emitted laser intensity which can be switched from low to high values. This behavior is explainable with the bend-induced change of the direction of the grating vector. It is important to underline that these are preliminary measurements. In Figure 7, we only reported the experimentally observed phenomena which certainly deserves a future deeper investigation.
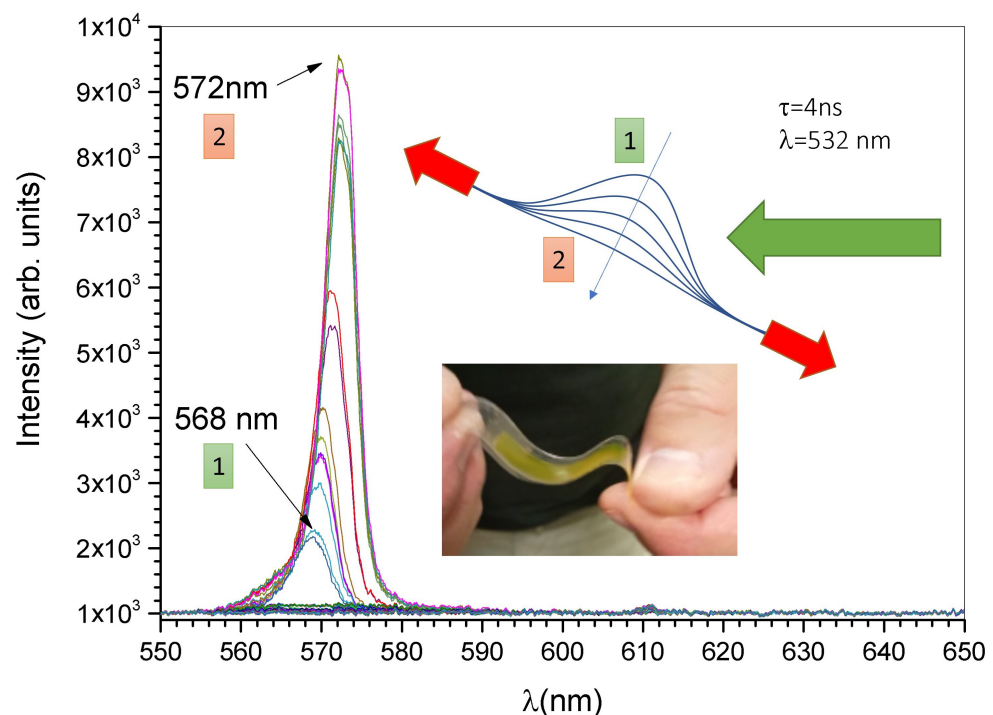
Figure 7. Demonstration of the tuning possibilities of the free-standing film. On the right side a sketch of the experimental setup. By stretching the film along the directions indicated by the red arrows, bending occurs and the emission can be tuned from 568 to 572 nm. The real device is shown in the inset.

4. Conclusions

In conclusion, a new holographic mixture is used to record phase reflection gratings showing very good diffraction efficiency values. The mixture containing the laser dye R6G can be optically pumped obtaining a lasing effect in a free-standing configuration. ASE effect and lasing are observed outside and inside the grating area. An interesting tunability of the ASE emission is reported. This flexible, stretchable, tunable, and switchable DFB-laser could open up new perspectives in the field of plastic organic laser devices.

Conflicts of Interest: The authors declare no conflict of interest.

References

1. He, J.; Zhao, Y.; Zhao, Y. Photoinduced bending of a coumarin-containing supramolecular polymer. *Soft Matter* **2009**, *5*, 308–310. [CrossRef]
2. Lucchetta, D.; Vita, F.; Francescangeli, D.; Francescangeli, O.; Simoni, F. Optical measurement of flow rate in a microfluidic channel. *Microfluid. Nanofluid.* **2016**, *20*, 9. [CrossRef]
3. Kondo, M.; Takemoto, M.; Fukae, R.; Kawatsuki, N. Photomobile polymers from commercially available compounds: Photoinduced deformation of side-chain polymers containing hydrogen-bonded photoreactive compounds. *Polym. J.* **2012**, *44*, 410–414. [CrossRef]
4. Lucchetta, D.; Spegni, P.; Di Donato, A.; Simoni, F.; Castagna, R. Hybrid surface-relief/volume one dimensional holographic gratings. *Opt. Mater.* **2015**, *42*, 366–369. [CrossRef]
5. Hu, Y.; Wu, G.; Lan, T.; Zhao, J.; Liu, Y.; Chen, W. A Graphene-Based Bimorph Structure for Design of High Performance Photoactuators. *Adv. Mater.* **2015**, *27*, 7867–7873.
6. Castagna, R.; Lucchetta, D.E.; Rippa, M.; Xu, J.H.; Donato, A.D. Near-frequency photons Y-splitter. *Appl. Mater. Today* **2020**, *19*, 100636. [CrossRef]
7. Zhang, X.; Yu, Z.; Wang, C.; Zarrouk, D.; Seo, J.W.T.; Cheng, J.C.; Buchan, A.D.; Takei, K.; Zhao, Y.; Ager, J.W.; et al. Photoactuators and motors based on carbon nanotubes with selective chirality distributions. *Nat. Commun.* **2014**, *5*, 2983. [CrossRef]
8. Lucchetta, D.; Simoni, F.; Hernandez, R.; Mazzulla, A.; Cipparrone, G. Lasing from chiral doped nematic liquid crystal droplets generated in a microfluidic device. *Mol. Cryst. Liq. Cryst.* **2017**, *649*, 11–19. [CrossRef]
9. Angeloni, A.S.; Caretti, D.; Carlini, C.; Chiellini, E.; Galli, G.; Altomare, A.; Solaro, R.; Laus, M. Photochromic liquid-crystalline polymers. Main chain and side chain polymers containing azobenzene mesogens. *Liq. Cryst.* **1989**, *4*, 513–527.
10. Kawatsuki, N.; Hasegawa, T.; Ono, H.; Tamoto, T. Formation of Polarization Gratings and Surface Relief Gratings in Photocrosslinkable Polymer Liquid Crystals by Polarization Holography. *Adv. Mater.* **2003**, *15*, 991–994. . adma.200304988. [CrossRef]
11. Shalit, A.; Lucchetta, D.; Piazza, V.; Simoni, F.; Bizzarri, R.; Castagna, R. Polarization-dependent laser-light structured directionality with polymer composite materials. *Mater. Lett.* **2012**, *81*, 232–234. [CrossRef]
12. De Sio, L.; Serak, S.; Tabiryan, N.; Ferjani, S.; Veltri, A.; Umeton, C. Composite Holographic Gratings Containing Light-Responsive Liquid Crystals for Visible Bichromatic Switching. *Adv. Mater.* **2010**, *22*, 2316–2319. [CrossRef] [PubMed]
13. Lucchetta, D.E.; Di Donato, A.; Singh, G.; Castagna, R. Lasing in Haloalkanes-based polymeric mixtures. *Opt. Mater.* **2022**, *131*, 112614. [CrossRef]
14. Karl, M.; Glackin, J.M.E.; Schubert, M.; Kronenberg, N.M.; Turnbull, G.A.; Samuel, I.D.W.; Gather, M.C. Flexible and Ultra-Lightweight Polymer Membrane Lasers. In Proceedings of the 2019 Conference on Lasers and Electro-Optics Europe & European Quantum Electronics Conference (CLEO/Europe-EQEC), Munich, Germany, 23–27 June 2019. [CrossRef]
15. Castro-Smirnov, J.; Sousaraei, A.; Osorio, M.; Casado, S.; Hernandez, J.J.; Wu, L.; Zhang, Q.; Xia, R.; Granados, D.; Wannemacher, R.; et al. Flexible distributed feedback lasers based on nanoimprinted cellulose diacetate with efficient multiple wavelength lasing. *NPJ Flex. Electron.* **2019**, *3*, 17. [CrossRef]
16. Castagna, R.; Lucchetta, D.; Vita, F.; Criante, L.; Greci, L.; Simoni, F. Haloalkane-based polymeric mixtures for high density optical data storage. *Opt. Mater.* **2008**, *30*, 1878–1882. [CrossRef]
17. Lucchetta, D.E.; Di Donato, A.; Francescangeli, O.; Singh, G.; Castagna, R. Light-Controlled Direction of Distributed Feedback Laser Emission by Photo-Mobile Polymer Films. *Nanomaterials* **2022**, *12*, 2890. [CrossRef]
18. Castagna, R.; Vita, F.; Lucchetta, D.E.; Criante, L.; Greci, L.; Ferraris, P.; Simoni, F. Nitroxide radicals reduce shrinkage in acrylate-based holographic gratings. *Opt. Mater.* **2007**, *30*, 539–544. [CrossRef]
19. Waldman, D.; Li, H.; Horner, M. Volume shrinkage in slant fringe gratings of a cationic ring-opening holographic recording material. *J. Imaging Sci. Technol.* **1997**, *41*, 497–514.
20. Castagna, R.; Davis, P.; Vasu, V.; Soucek, K.; Cross, C.; Greci, L.; Valacchi, G. Nitroxide radical TEMPO reduces ozone-induced chemokine IL-8 production in lung epithelial cells. *Toxicol. Vitr.* **2009**, *23*, 365–370. [CrossRef]
21. Ramos, G.; Álvarez-Herrero, A.; Belenguer, T.; del Monte, F.; Levy, D. Shrinkage control in a photopolymerizable hybrid solgel material for holographic recording. *Appl. Opt.* **2004**, *43*, 4018–4024. [CrossRef]
22. Peters, G.I.; Allen, L. Amplified spontaneous emission I. The threshold condition. *J. Phys. A Gen. Phys.* **1971**, *4*, 238. [CrossRef]
23. McGehee, M.D.; Gupta, R.; Veenstra, S.; Miller, E.K.; Díaz-García, M.A.; Heeger, A.J. Amplified spontaneous emission from photopumped films of a conjugated polymer. *Phys. Rev. B* **1998**, *58*, 7035–7039. [CrossRef]
24. Malcuit, M.S.; Maki, J.J.; Simkin, D.J.; Boyd; W, R. Transition from superfluorescence to amplified spontaneous emission. *Phys. Rev. Lett.* **1987**, *59*, 1189–1192. [CrossRef] [PubMed]

25. Ganiel, U.; Hardy, A.; Neumann, G.; Treves, D. Amplified spontaneous emission and signal amplification in dye-laser systems. *IEEE J. Quantum Electron.* **1975**, *11*, 881–892. [CrossRef]

26. Eichler, H.; Günter, P.; Pohl, D. *Laser-Induced Dynamic Gratings*; Springer Series in Optical Sciences; Springer: Berlin/Heidelberg, Germany, 2013.

27. Kneubühl, F. *Theories on Distributed Feedback Lasers*; Handbook of laser science and technology; Harwood Academic Publishers: Reading, UK, 1993.

28. Criante, L.; Lucchetta, D.; Vita, F.; Castagna, R.; Simoni, F. Distributed feedback all-organic microlaser based on holographic polymer dispersed liquid crystals. *Appl. Phys. Lett.* **2009**, *94*, 111114. [CrossRef]

29. Fu, Y.; Zhai, T. Distributed feedback organic lasing in photonic crystals. *Front. Optoelectron.* **2020**, *13*, 18–34. [CrossRef]

30. Zhai, T.; Ma, X.; Han, L.; Zhang, S.; Ge, K.; Xu, Y.; Xu, Z.; Cui, L. Self-Aligned Emission of Distributed Feedback Lasers on Optical Fiber Sidewall. *Nanomaterials* **2021**, *11*, 2381. [CrossRef]

31. Kok, M.H.; Lu, W.; Lee, J.C.W.; Tam, W.Y.; Wong, G.K.; Chan, C.T. Lasing from dye-doped photonic crystals with graded layers in dichromate gelatin emulsions. *Appl. Phys. Lett.* **2008**, *92*, 151108. [CrossRef]